PARAMETER STUDY OF UNDERGROUND AMMUNITION STORAGE MAGAZINES: RESULTS OF EXPLOSION TESTS IN SMALL-SCALE MODELS

Charles E. Joachim
Christo V. Lunderman

U.S. Army Engineer Waterways Experiment Station
Vicksburg, MS

A series of 1:20-scale model tests were conducted to investigate the effects of tunnel diameter, tunnel length, and chamber loading density on the Airblast Inhabited Building Distance (IBD) from accidental explosions in underground magazines. The results indicate that the IBD decreases, to different degrees, with increased tunnel diameter, decreased loading density, or increased tunnel length. The analysis shows that these effects are primarily a function of the total volume of the underground system.

INTRODUCTION

The U.S. Army Engineer Waterways Experiment Station (WES) has conducted research on airblast propagation inside underground ammunition storage facilities. The purpose of the research was to develop magazine design enhancements which would minimize the Airblast Inhabited Building Distance (IBD) should an accidental internal detonation occur. This effort was a part of the Joint U.S./Korea R&D Study for New Underground Ammunition Storage Technologies.

A series of 1:20-scale experiments were conducted at WES to establish a baseline data base against which to evaluate the effects of blast reduction designs on the IBD. Parameters evaluated during the study included tunnel length, tunnel/chamber diameter ratio, and chamber loading density (Table l). The parameter study was performed with a simple, "shot gun" design of an underground magazine (storage chamber and access tunnel coaxially aligned).

DESCRIPTION OF THE MODEL

The small-scale model consisted of a detonation chamber and exit tunnel. The detonation chamber was fabricated from a 50.8 cm (inside diameter) steel pipe and rings of steel plate (7.6 cm thick), and had an outer diameter of 81.3 cm. The exit tunnel was made of heavy-walled steel pipe, with inside diameters 0.3, 0.5, and 0.7 times the chamber diameter.

Explosive charges for the model tests were assembled from blocks of Composition C-4. Nominal dimensions of the basic charge blocks were 5.08 cm wide, by 2.54 cm thick, by 22.5

Report Documentation Page

Form Approved
OMB No. 0704-0188

1. REPORT DATE **AUG 1994**	2. REPORT TYPE	3. DATES COVERED **00-00-1994 to 00-00-1994**
4. TITLE AND SUBTITLE **Parameter Study of Underground Ammunition Storage Magazines: Results of Explosion Tests in Small-Scale Models**		5a. CONTRACT NUMBER 5b. GRANT NUMBER 5c. PROGRAM ELEMENT NUMBER
6. AUTHOR(S)		5d. PROJECT NUMBER 5e. TASK NUMBER 5f. WORK UNIT NUMBER
7. PERFORMING ORGANIZATION NAME(S) AND ADDRESS(ES) **U.S. Army Engineer Waterways Experiment Station,3909 Halls Ferry Road,Vicksburg,MS,39180-6199**		8. PERFORMING ORGANIZATION REPORT NUMBER
9. SPONSORING/MONITORING AGENCY NAME(S) AND ADDRESS(ES)		10. SPONSOR/MONITOR'S ACRONYM(S) 11. SPONSOR/MONITOR'S REPORT NUMBER(S)
12. DISTRIBUTION/AVAILABILITY STATEMENT **Approved for public release; distribution unlimited**		
13. SUPPLEMENTARY NOTES **See also ADM000767. Proceedings of the Twenty-Sixth DoD Explosives Safety Seminar Held in Miami, FL on 16-18 August 1994.**		
14. ABSTRACT		
15. SUBJECT TERMS		

16. SECURITY CLASSIFICATION OF:			17. LIMITATION OF ABSTRACT	18. NUMBER OF PAGES	19a. NAME OF RESPONSIBLE PERSON
a. REPORT **unclassified**	b. ABSTRACT **unclassified**	c. THIS PAGE **unclassified**	**Same as Report (SAR)**	**14**	

Standard Form 298 (Rev. 8-98)
Prescribed by ANSI Std Z39-18

cm long, and weighed 0.609 kg. The explosive blocks were stacked to provide explosive loading densities (charge weight per cubic meter of chamber volume) of 1.67, 3.33, and 5.00 kg/m^3. The charges were positioned at the center of the chamber, supported on a light wire frame. An RP-83 electric bridge wire (EBW) detonator embedded in the end of the C-4 charge (end closest to the exit tunnel) initiated the explosive charge.

Instrumentation to measure the airblast pressures consisted of airblast gages located along the interior surface of the detonation chamber and exit tunnel, and external airblast pressure gages located on the ground surface outside the portal, along the extended centerline of the exit tunnel. Kulite Corporation Model HKS-375 pressure transducers were used for the internal airblast measurements. The internal gages were flush-mounted on the inner wall of the detonation chamber and pipe sections (side-on pressure measurements) . These gages had dynamic ranges of 210 MPa to 3.4 MPa, with associated resonant frequencies of 725 to 650 kHz.

The external measurements employed Kulite Model XT-l90 airblast gages. These instruments had dynamic ranges between 13.8 MPa and 35 kPa, and associated resonant frequencies between 650 kHz and 70 kHz. The free-field gages were mounted flush to the ground surface beyond the tunnel exits at ranges (from the exit) of 1.8, 3.0, 4.8, and 8.0 m.

BLASTX3 CALCULATIONS

A computational model of the small-scale experiments was developed using BLASTX3, a WES-developed, empirical-based airblast code. This code has undergone a recent revision to allow calculation of airblast propagation in tunnels for moderate to large loading densities. Data from the WES small-scale model test program and one-dimensional hydrocode calculations were used in developing the improved version of the code (BLASTX3).

Two experiments (Series l, Tests 9 and 21), both with tunnel/chamber diameter ratio's of 0.5 and chamber explosive loading densities of 5 kg/m^3, were calculated with the BLASTX3 computational model. The length of the exit tunnels were 2 m (Test 9) and 4 m (Test 21). The physical model was divided into cylindrical sections with an approximate length to diameter aspect ratio of 3:1 for the computational model. The length-to-diameter ratio of the model detonation chamber was 3.5 to 1. For the computation model, the chamber was modeled as a single cylindrical room. Similarly, the exit tunnels were divided into 3 (Test 9) and 6 (Test 21) equal cylindrical sections in the computational model.

Since BLASTX3 can only model spherical charges, the rectangular parallelepiped explosive charge used in the physical experiments was represented by a single spherical charge int he computation.

RESULTS OF EXPERIMENTS AND CALCULATIONS

From the small-scale experiments, the normalized peak overpressure data recorded in the free-field beyond the tunnel portal are plotted versus normalized distance in Figures 2 through 8. The non-dimensional pressure values were obtained by dividing the calculated effective exit pressure by the measured peak free-field pressure (DDESB, 1993). The effective exit pressure (P_w) is calculated from

EQUATION

$$P_w = 1770.5 \left[\frac{Q}{V_t}\right]^{\frac{1.35}{3}}$$

where

Q is the net explosive weight in the chamber, kg, and V_t is the total volume of the underground storage system, m^3.

The normalized distances were computed by dividing the distances from the exit portal by the hydraulic tunnel diameter for turbulent flow, which is obtained from

$$D = \frac{4A}{P}$$

where

A is the minimum cross-sectional area of the tunnel, m^2, and P is the perimeter of the minimum tunnel cross-section, m.

The equation developed by the DOD Explosives Safety Board (DDESB) to predict the normalized IBD is included in Figures 2 through 8 to provide a reference against which to evaluate the experimental data. The normalized IBD prediction relation is

$$\frac{P_v}{P} = (R/D)^{1.35}$$

where

P is the peak free-field overpressure, kPa, and R is the distance from the portal, m.

Although there is some data scatter, the normalized free-field pressure shows no significant influence of the chamber loading density (Figures 2, 3, and 4, respectively. As shown in these graphs, the trend of the experimental data follows the IBD prediction line. The normalized peak pressures in the free-field as calculated by BbASTX3 are also shown in Figure 3, (for the 5.00 kg/m^3 loading density). The BLASTX3 curve follows the trend of the data (triangles) for this loading density.

The effect of tunnel length on normalized free-field overpressure is shown in Figures 5, 6, and 7. Although the experimental results exhibit some scatter, no significant influence of tunnel length can be identified from these test results. Figure 6 shows the normalized overpressures calculated by BThASTX3, for 2 an 4-m tunnel lengths. The BLASTX3 results indicate decreased free-field pressures with increased tunnel lengths.

A comparison of data from the three tunnel/chamber diameter ratios that were evaluated in the small-scale test program is shown in Figure 8. The data exhibits some scatter, masking any effects of tunnel diameter. Base on these results, the effect of tunnel diameter on free-field pressures (and the IBD) was judged to be insignificant.

As mentioned earlier, the total volume of the underground magazine system was used to calculate the effective exit pressure. In effect, normalizing the free-f ield pressure data with the effective exit pressure accounts for the extra volumes associated with larger or longer access tunnels. Similarly, the effective exit pressure calculation includes the charge weight or mass. Thus, the normalizing procedure essentially eliminates the effect of loading density from the data comparisons presented in this paper. Therefore, a doubling of the explosive load in an underground magazine should increase the free-field pressures by a factor of two taken to the 0.45 power.

CONCLUSIONS

The results of explosive tests conducted in 1:20-scale models provided indications of the extent to which the IBD decreases as a function of increased tunnel diameter and tunnel length, and decreased loading density. However, when the peak airblast pressures are normalized and plotted against normalized distance from the tunnel portal (using current DDESB formulas for normalizing these parameters), there is no significant, independent effect of chamber loading density, tunnel length, or tunnel diameter. These conclusions were supported by the results of calculations using the BLASTX3 computer model.

ACKNOWLEDGMENT

We appreciate the cooperation of the authorities at the Geomechanics and Explosion Effects Division, Structures Laboratory, U.S. Army Engineers Waterways Experiment Station and the Headquarters, U.S. Army Corps of Engineers that permitted us to prepare and present this paper for publication.

REFERENCES

Department of Defense, 1991, "Ammunition and Explosives Safety Standards," DOD 6055.9-STD, Assistant Secretary of Defense (Manpower, Installations, and Logistics), Washington, D.C.

TABLE 1. JOINT U.S./ROK R&D PROGRAM FOR NEW UNDERGROUND AMMUNITION STORAGE TECHNOLOGIES: SMALL-SCALE MODEL TEST PARAMETERS

TEST NO.	VENT PIPE LENGTH (m)	TUNNEL/CHAMBER DIAMETER RATIO	LOADING DENSITY (kg/m^3)
1	1	0.3	1.67
2	1	0.3	3.33
3	1	0.3	5.00
4	2	0.3	1.67
5	2	0.3	3.33
6	2	0.3	5.00
7	2	0.5	1.67
8	2	0.5	3.33
9	2	0.5	5.00
10	2	0.7	1.67
11	2	0.7	3.33
12	2	0.7	5.00
13	1	0.7	1.67
14	1	0.7	3.33
15	1	0.7	5.00
16	1	0.5	1.67
17	1	0.5	3.33
18	1	0.5	5.00
19	4	0.5	1.67
20	4	0.5	3.33
21	4	0.5	5.00
22	4	0.7	1.67
23	4	0.7	3.33
24	4	0.7	5.00
25	4	0.3	1.67
26	4	0.3	3.33
27	4	0.3	5.00

TABLE 1. JOINT U.S./ROK R&D PROGRAM FOR NEW UNDERGROUND AMMUNITION STORAGE TECHNOLOGIES: SMALL-SCALE MODEL TEST PARAMETERS

FIGURE 1.
CONTROL MAGAZINE TEST SERIES, PLAN VIEW OF GENERIC TEST LAYOUT. VENT PIPE LENGTHS RANGED FROM 1 TO 4 M.

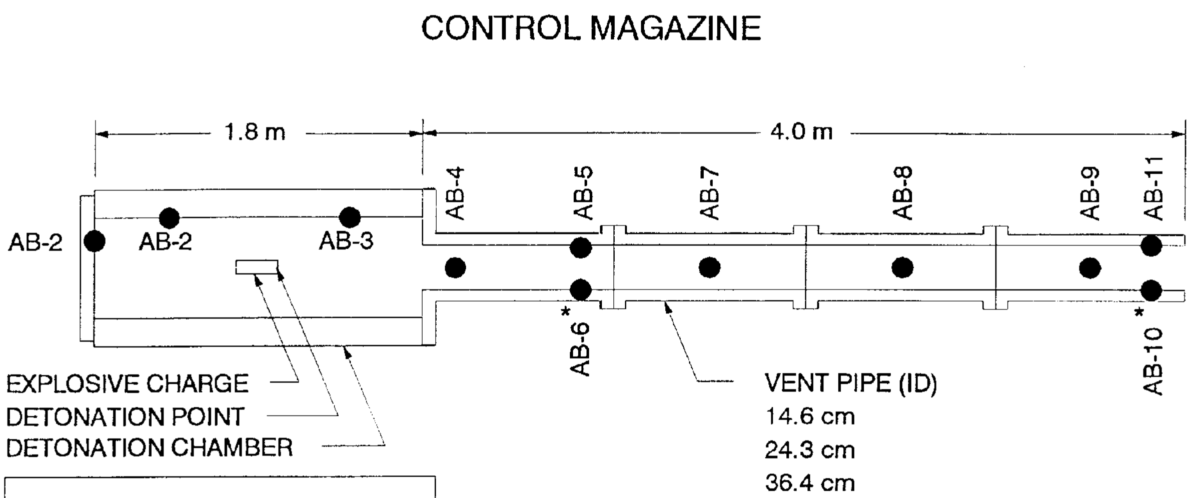

FREE-FIELD GAGE LOCATIONS

GAGE NO.	DISTANCE FROM PORTAL m
AB-12	1.8
AB-13	3.0
AB-14 *	3.0
AB-15	4.8
AB-16 *	4.8
AB-17	8.0
AB-18 *	8.0

Note: * denotes stagnation pressure measurement gage placed surface flush 1.3 cm in front of 2.5 cm cube

Figure 1. Control magazine test series, plan view of generic test layout. Vent pipe lengths ranged from 1 to 4 m.

Figure 2. Effect of loading density: comparison of normalized peak free-field overpressure from small-scale model tests at chamber loading densities of 1.67, 3.33, and 5.00 kg/m^3 for a tunnel/chamber diameter ratio of 0.3, and tunnel length of 4 m.

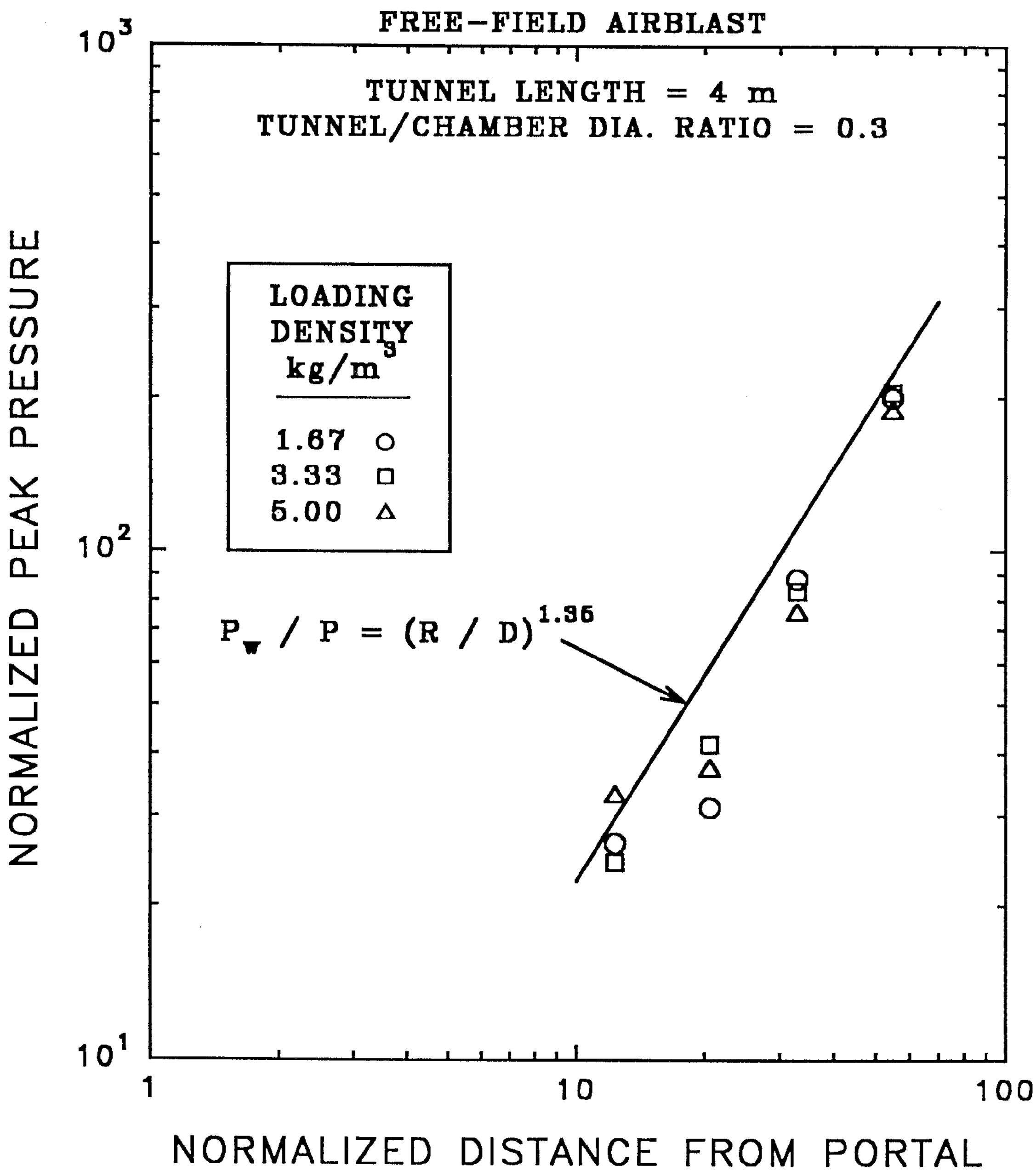

Figure 2. Effect of loading density: comparison of normalized peak free-field overpressure from small-scale model tests at chamber loading densities of 1.67, 3.33, and 5.00 kg/m^3 for a tunnel/chamber diameter ratio of 0.3, and tunnel length of 4 m.

Figure 3. Effect of loading density: comparison of normalized peak free-field overpressure from small-scale model tests at chamber loading densities of 1.67, 3.33, and 5.00 kg/m^3 for a tunnel/chamber diameter ratio of 0.5, and tunnel length of 4 m.

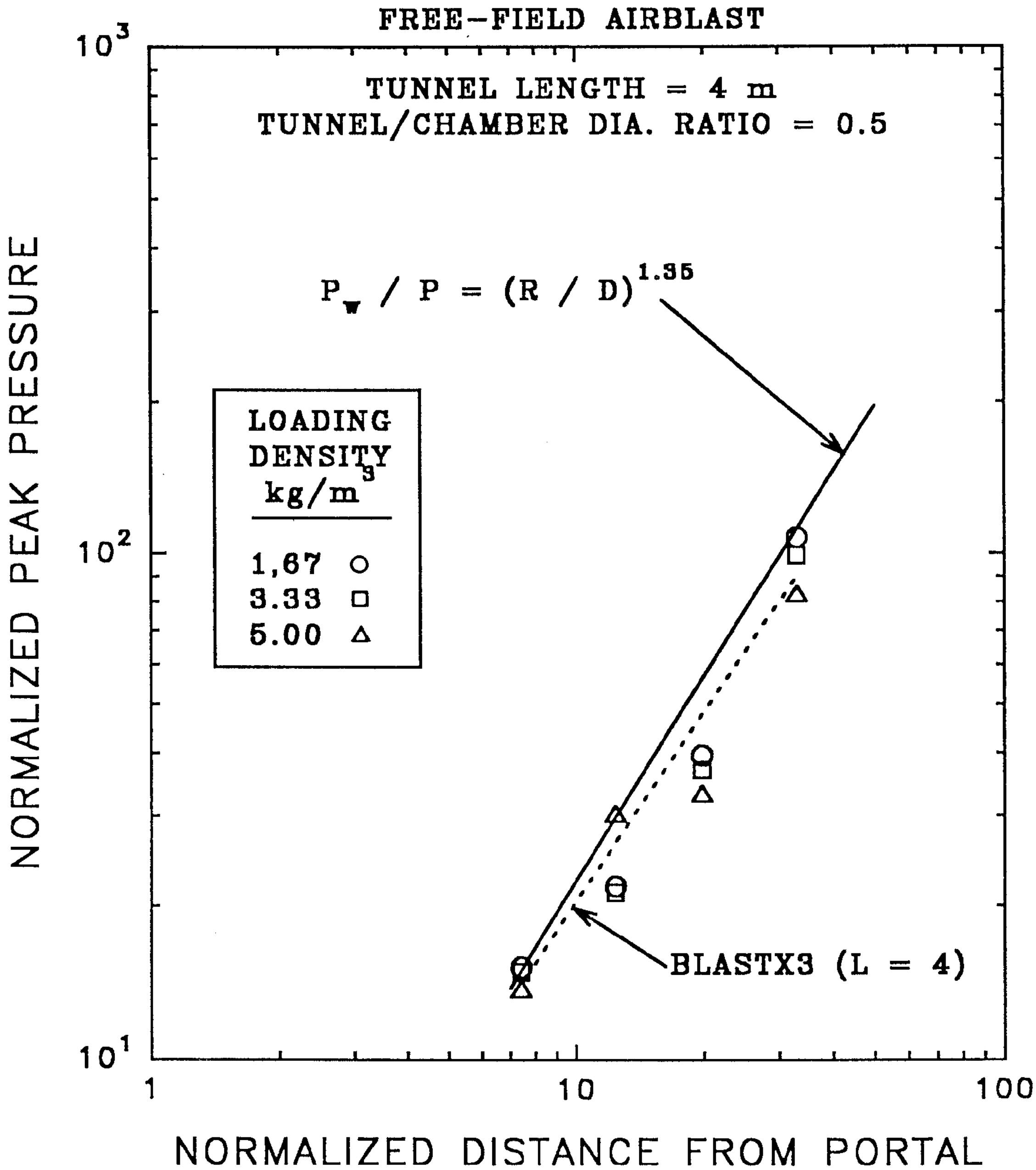

Figure 3. Effect of loading density: comparison of normalized peak free-field overpressure from small-scale model tests at chamber loading densities of 1.67, 3.33, and 5.00 kg/m^3 for a tunnel/chamber diameter ratio of 0.5, and tunnel length of 4 m.

Figure 4. Effect of loading density: comparison of normalized peak free-field overpressure from small-scale model tests at chamber loading densities of 1.67, 3.33, and 5.00 kg/m^3 for a tunnel/chamber diameter ratio of 0.7, and tunnel length of 4 m.

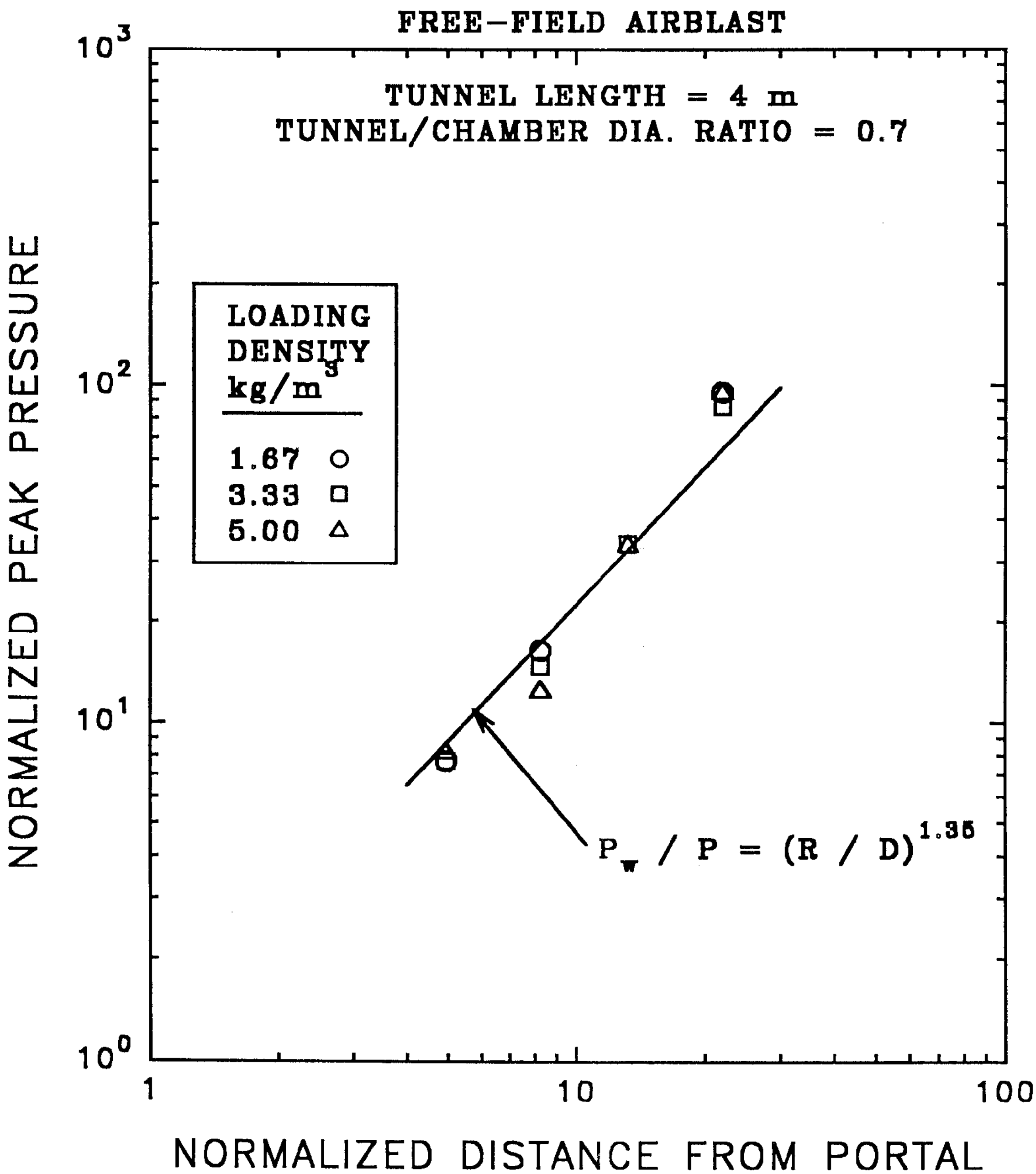

Figure 4. Effect of loading density: comparison of normalized peak free-field overpressure from small-scale model tests at chamber loading densities of 1.67, 3.33, and 5.00 kg/m^3 for a tunnel/chamber diameter ratio of 0.7, and tunnel length of 4 m.

Figure 5. Effect of tunnel length: comparison of normalized peak free-field overpressure from small-scale model tests with access tunnel lengths of l, 2, and 4 m for a chamber loading density of 5.00 kg/m³ and a tunnel/chamber diameter ratio of 0.3.

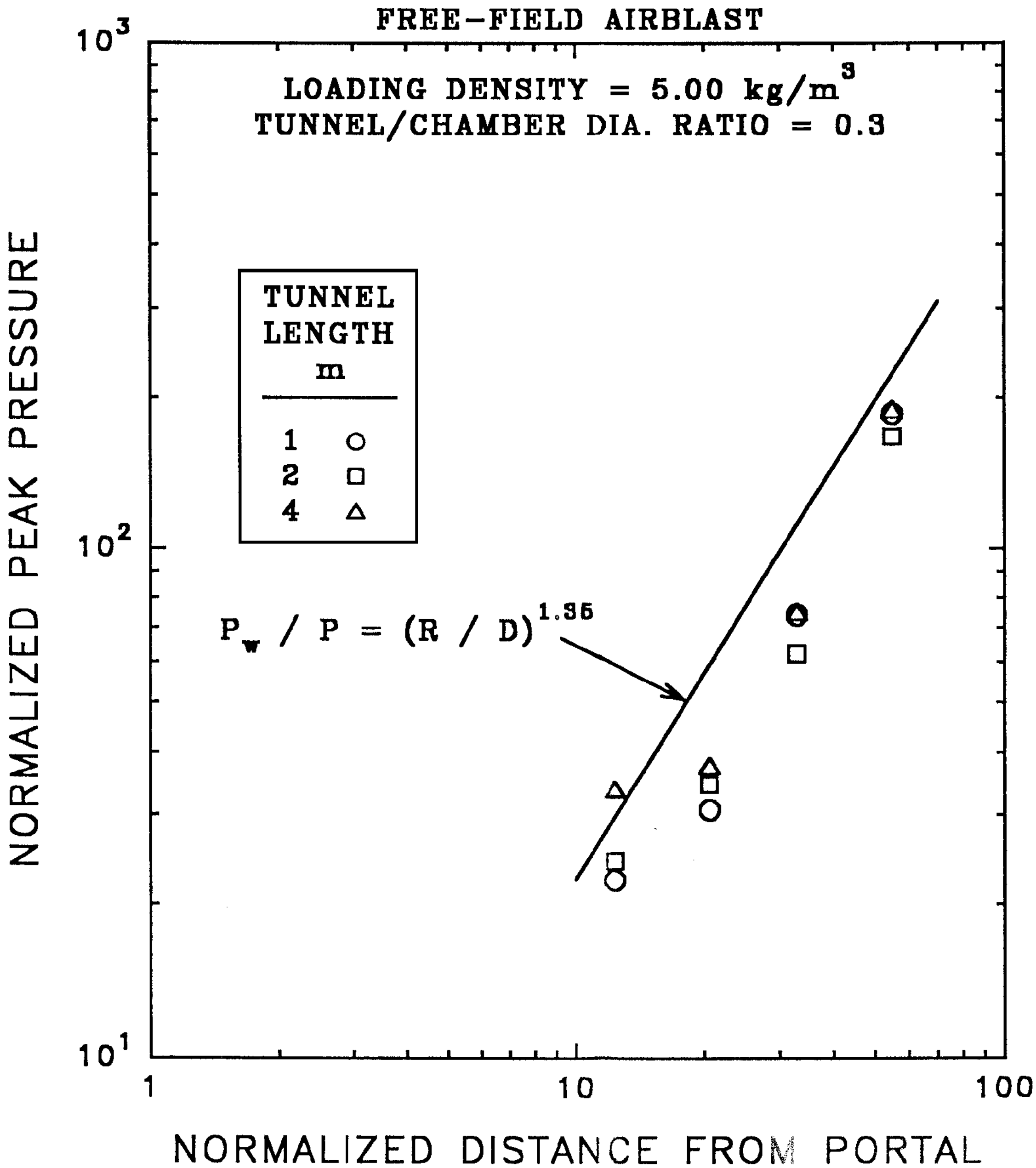

Figure 5. Effect of tunnel length: comparison of normalized peak free-field overpressure from small-scale model tests with access tunnel lengths of 1, 2, and 4 m for a chamber loading density of 5.00 kg/m³ and a tunnel/chamber diameter ratio of 0.3.

Figure 6. Effect of tunnel length: comparison of normalized peak free-field overpressure from small-scale model tests with access tunnel lengths of 1, 2, and 4 m for a chamber loading density of 5.00 kg/m^3 and a tunnel/chamber diameter ratio of 0.5.

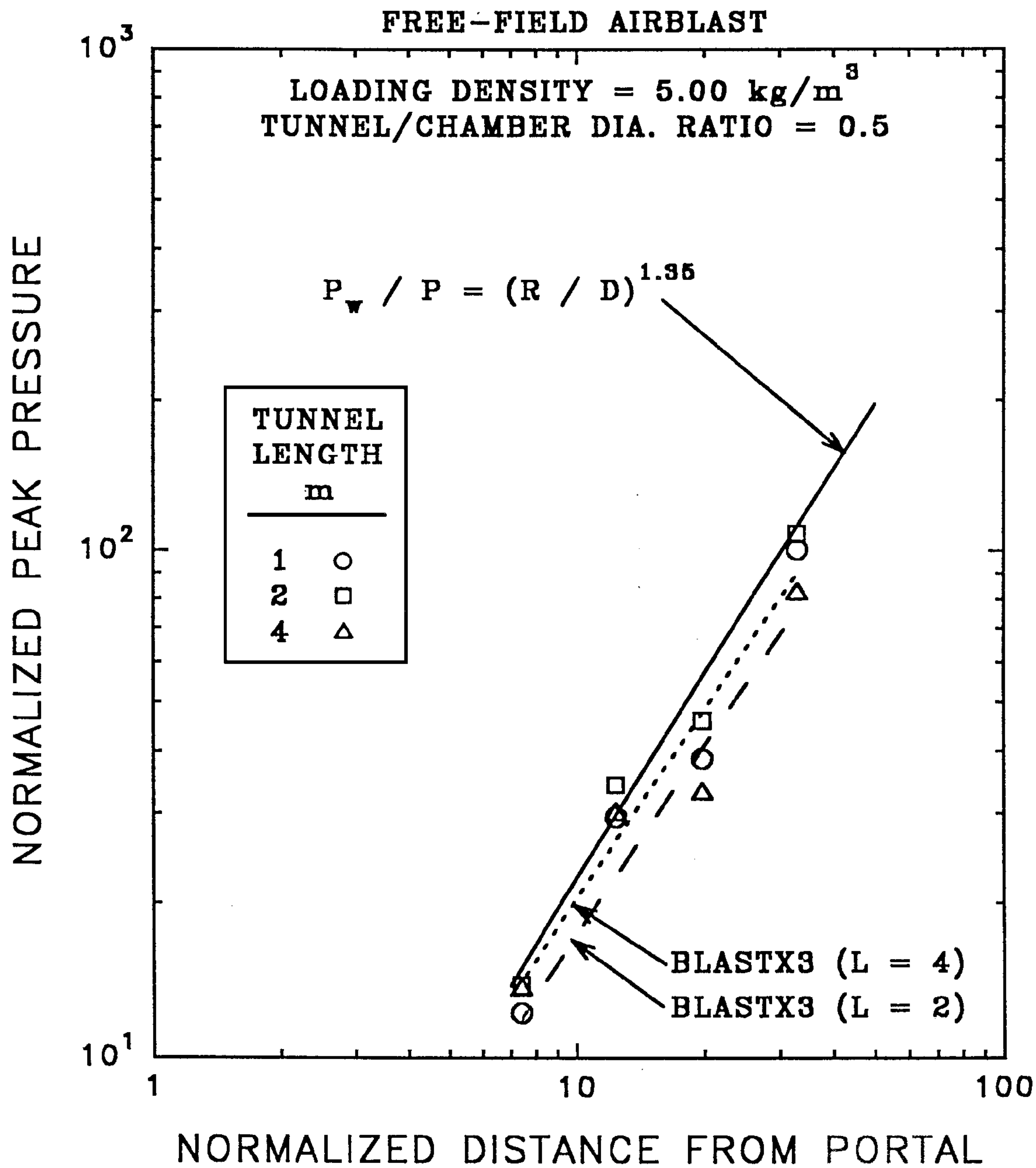

Figure 6. Effect of tunnel length: comparison of normalized peak free-field overpressure from small-scale model tests with access tunnel lengths of 1, 2, and 4 m for a chamber loading density of 5.00 kg/m^3 and a tunnel/chamber diameter ratio of 0.5.

Figure 7. Effect of tunnel length: comparison of normalized peak free-f ield overpressure from small-scale model tests with access tunnel lengths of 11 2, and 4 m for a chamber loading density of 5.00 kg/m^3 and a tunnel/chamber diameter ratio of 0.7.

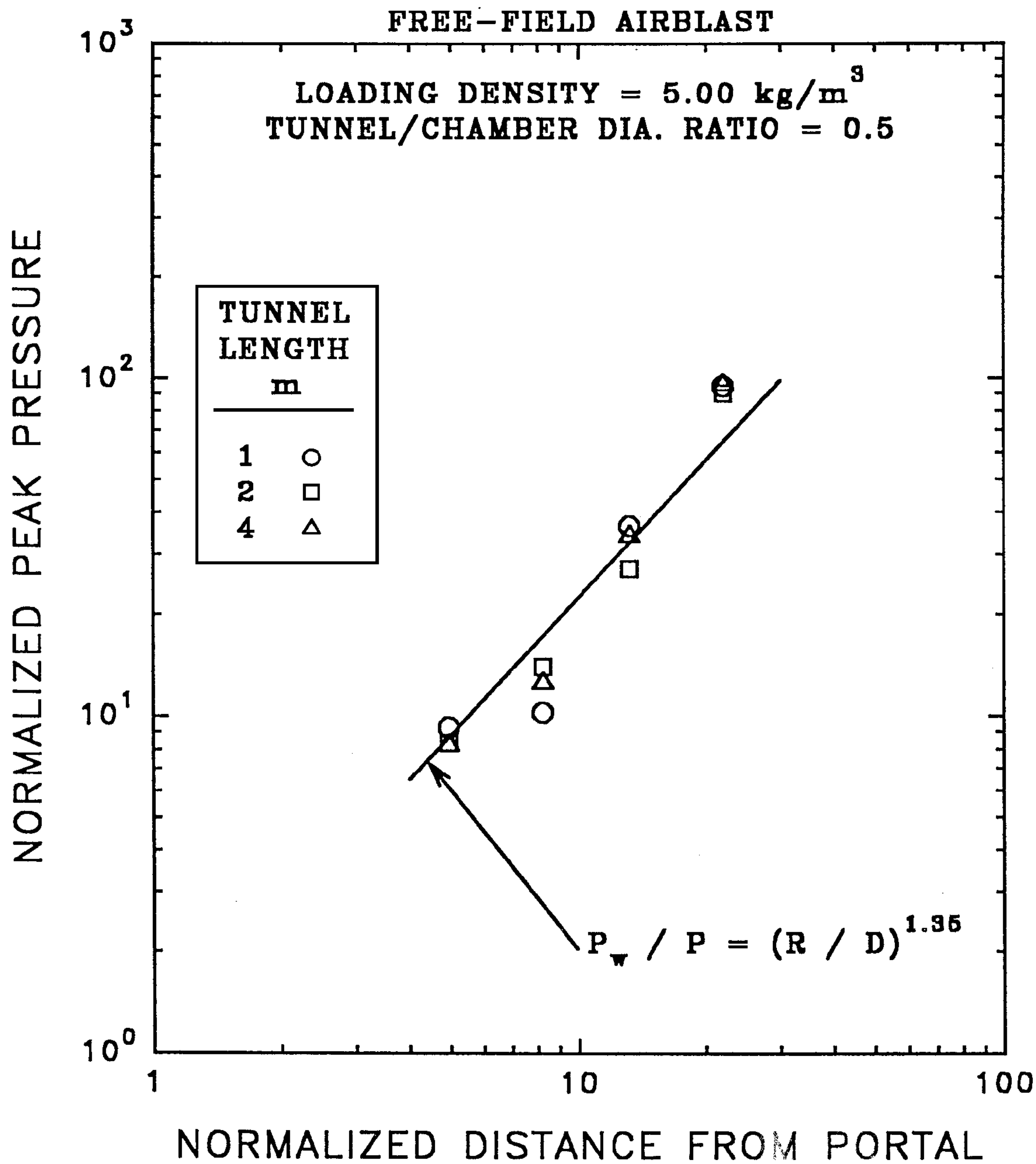

Figure 7. Effect of tunnel length: comparison of normalized peak free-field overpressure from small-scale model tests with access tunnel lengths of 1, 2, and 4 m for a chamber loading density of 5.00 kg/m^3 and a tunnel/chamber diameter ratio of 0.7.

Figure 8. Effect of tunnel/chamber diameter ratio: comparison of normalized peak free-field overpressure from smallscale tests with tunnel/chamber diameter ratio's of 0.3, 0.5, and 0.7 for a chamber loading density of 5.00 kg/m^3 and tunnel length of 4 m.

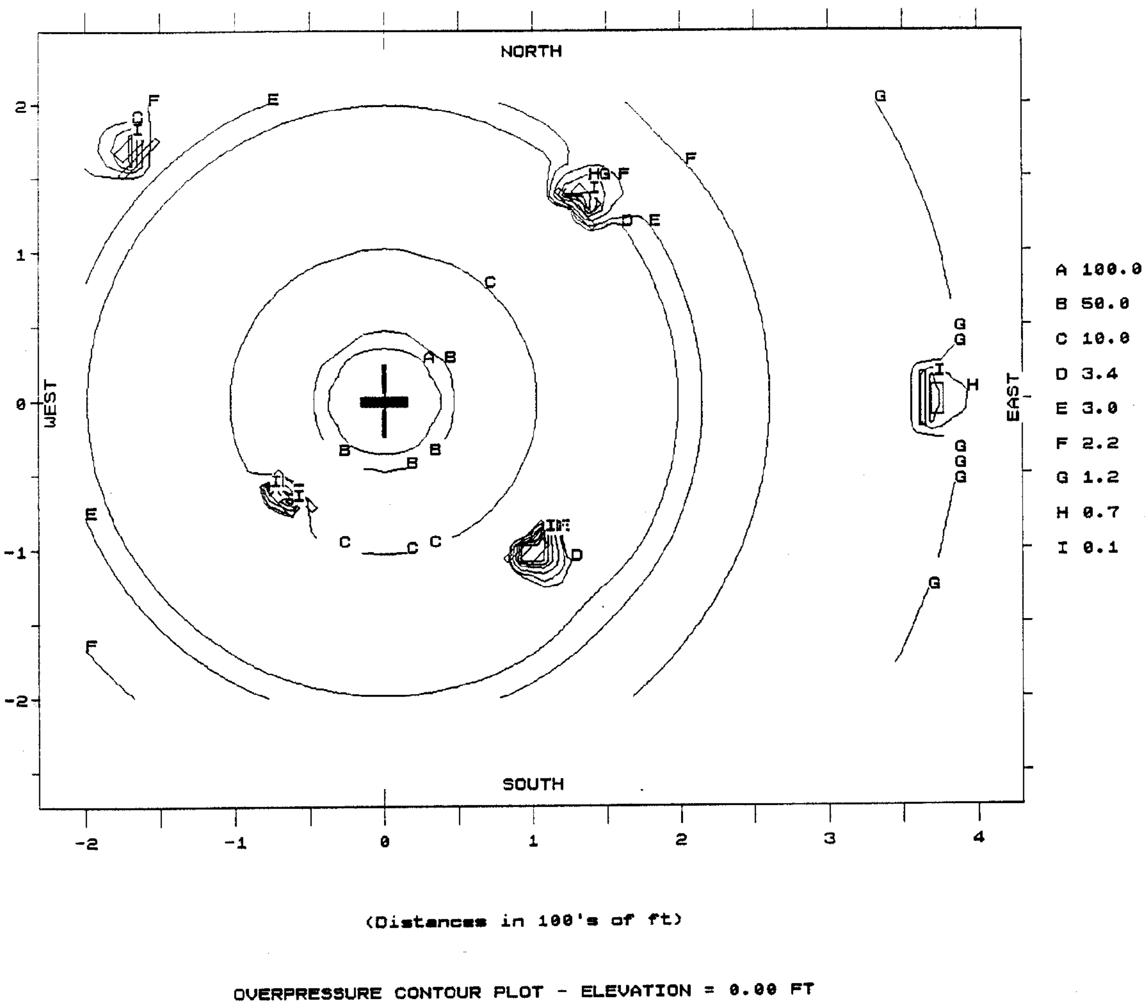

Figure 8 Overpressure generated (in psi) when sandbags are used.